Workshop 1: Airframe Flutter

Aeroservoelasticity 2024/2025 - Prof. Quaranta

Team members	Personal code
Matteo Baio	10667431
Gaia Lapucci	10710434
Lorenzo Lucatello	10735694

Introduction

The aim of this workshop is to visualize and analyze the aeroelastic behavior of a semiwing model of the XV-15 tiltrotor. The whole dissertation will be divided in different tasks that, step by step, starting from an initial finite element model, will lead to a final and complete aeroelastic model used to perform a flutter analysis.

Input Data

The starting point is the given finite element model defined by 47 nodes and the respective connectivity elements, both provided with nodes and elements label. The modal mass matrix $\mathbf{M}_{hh}$, the modal stiffness matrix $\mathbf{K}_{hh}$ and the eigenvectors are given as well. The model has 14 modes and for each mode the associated eigenvector is in the form of a 6×47 matrix, as we consider 6 degrees of freedom (3 translations and 3 rotations) for each node. The geometrical data of the semiwing are available in Table 1.

Span	9.8 m
Chord	1.6 m
Sweep	$-6.5°$
Dihedral	$2°$

Table 1: Geometrical data of the semiwing

To integrate aerodynamics in the structural model, we are going to use the aerodynamics state space matrices, which are also provided as input data.

Task 1: Plot the finite element model

With the provided Matlab function `meshVisualization.m` we were able to create the visualization of the FEM model as shown in Figure 1.

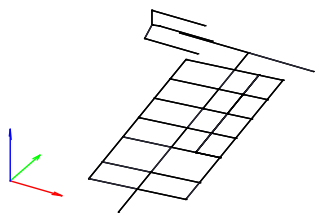

Figure 1: Finite element model

Task 2: Plot the mode shapes

Starting from the $\mathbf{\Phi}$ matrices that contain the eigenvectors for each mode and reorganizing it into a vector as displacement input for the `meshVisualization.m` function, we can visualize the modal shapes of the initial structural model.

Using the modal matrices $\mathbf{M}_{hh}$ and $\mathbf{K}_{hh}$ and solving the associated generalized eigenvalue problem with the MATLAB® function `eig( )`, eigenfrequencies can be computed as well and are reported in Table 2.

Mode	1	2	3	4	5	6	7
Frequency [Hz]	0	3.71	5.87	13.85	15.05	29.00	31.40

Table 2: Eigenfrequencies (Modes 1 to 7)

Mode	8	9	10	11	12	13	14
Frequency [Hz]	40.63	44.16	65.27	83.77	91.77	96.28	99.84

Table 3: Eigenfrequencies (Modes 8 to 14)

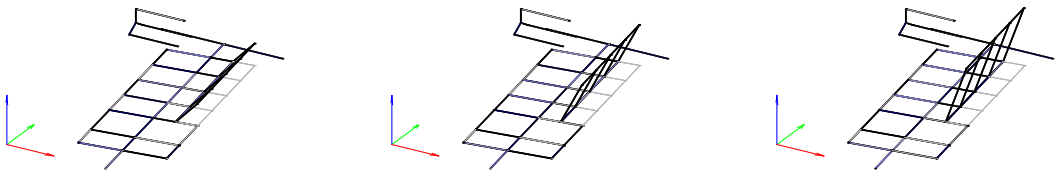

Figure 2: First Mode Shape

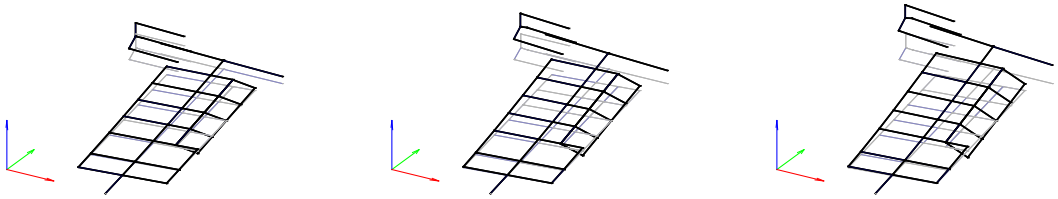

Figure 3: Second Mode Shape

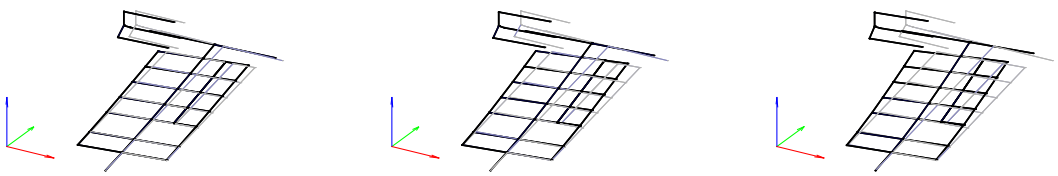

Figure 4: Third Mode Shape

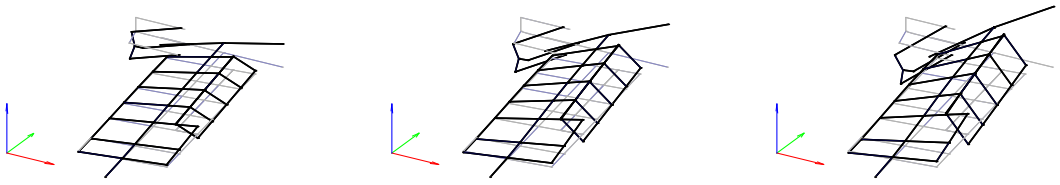

Figure 5: Fourth Mode Shape

As known, the most significant mode shapes are the first ones thanks to their low frequency content and their ability to capture the dynamic behavior of the structure. In this case, the first four are relevant since they are associated to almost uncoupled motions of the structure.

In fact, as can be seen in Figure 2, the shape of the first mode is, as expected, a rigid rotation of the aileron. This behavior is supported by the fact that the aileron is not restrained and therefore free to rotate. This is also confirmed also by the 0 frequency in Table 2.

The second and third mode shapes are, respectively, pure out-of-plane bending (Figure 3) and pure in-plane bending (Figure 4). The fourth is not a completely uncoupled mode because it is mainly a torsional mode with a small component of out-of-plane bending (Figure 5). A tiny rotation of the aileron can be appreciated in the last three cases as a part from the third modal shape. That is due to the fact that the degree of freedom associated to the movable surface (that is, torsional) is not connected to in-plane motion.

Task 3: Mode shapes with actuator stiffness

The first step was to determine on what degrees of freedom the actuator stiffness acts upon and, accordingly, develop the stiffness matrix for the actuator stiffness in the local reference frame.

We know that the actuator is placed on nodes 1205 and 2205 (node 2205 is on the aileron side, while node 1205 is on the wing side) and acts upon the rotational degree of freedom around the hinge line, which corresponds to the $\hat{y}$-axis (local reference frame). Therefore, considering only the 3 rotational degrees of freedom for each node and considering the self and mutual influence of the nodes, we build the following stiffness matrix:

$$\mathbf{K}_{\mathrm{act}_{\mathrm{local}}} = \underbrace{\begin{bmatrix} 0 & 0 & 0 & 0 & 0 & 0 \\ 0 & \mathrm{K_{act}} & 0 & 0 & -\mathrm{K_{act}} & 0 \\ 0 & 0 & 0 & 0 & 0 & 0 \\ 0 & 0 & 0 & 0 & 0 & 0 \\ 0 & -\mathrm{K_{act}} & 0 & 0 & \mathrm{K_{act}} & 0 \\ 0 & 0 & 0 & 0 & 0 & 0 \end{bmatrix}}_{\begin{array}{cc}\text{Node 1205} & \text{Node 2205}\end{array} \quad \begin{array}{l}\left.\vphantom{\begin{bmatrix}0\\0\\0\end{bmatrix}}\right\} \text{Node 1205} \\ \left.\vphantom{\begin{bmatrix}0\\0\\0\end{bmatrix}}\right\} \text{Node 2205}\end{array}$$

The second step is to express the matrix components from the local reference frame into the global one. Indeed, the actuator stiffness acts with respect to the hinge line, therefore affected by the wing sweep and wing dihedral. First we define the the rotation matrices about the x and z axis, which respectively represent the rotation of the hinge line due to the sweep and dihedral angles.

$$\mathbf{R}_{\mathrm{sweep}} = \begin{bmatrix} \cos\Lambda & -\sin\Lambda & 0 \\ \sin\Lambda & \cos\Lambda & 0 \\ 0 & 0 & 1 \end{bmatrix} \qquad \mathbf{R}_{\mathrm{dihedral}} = \begin{bmatrix} 1 & 0 & 0 \\ 0 & \cos\Gamma & -\sin\Gamma \\ 0 & \sin\Gamma & \cos\Gamma \end{bmatrix}$$

The overall rotation matrix that allow to change the reference from the local reference to the global reference will be:

$$\mathbf{R}_T = \mathbf{R}^T_{\mathrm{dihedral}}\,\mathbf{R}^T_{\mathrm{sweep}}$$

The stiffness matrix in the rotated reference frame will be computed by rotating the reference of the 3 rotational degrees of freedom associated with each node (rotating the 3×3 sub matrices of the $\mathbf{K}_{act_{local}}$ matrix).
The final step is to then assemble the new complete stiffness matrix. First we need to project the matrix into the modal coordinates. To do so we extract from the eigenvectors the ones associated with rotational degrees of freedom of nodes 1205 and 2205 and then apply the following transformation:

$$\mathbf{K}_{\text{hha}} = \begin{bmatrix} \boldsymbol{\phi}_{\text{rot}_{1205}} \\ \boldsymbol{\phi}_{\text{rot}_{2205}} \end{bmatrix}^T \mathbf{K}_{\text{act}_{\text{global}}} \begin{bmatrix} \boldsymbol{\phi}_{\text{rot}_{1205}} \\ \boldsymbol{\phi}_{\text{rot}_{2205}} \end{bmatrix}$$

To compute the overall modal stiffness matrix we sum the actuator modal stiffness matrix to the previous modal stiffness matrix.

$$\mathbf{K}_{\text{new}} = \mathbf{K}_{hh} + \mathbf{K}_{hha}$$

The last step is to then compute the modal shapes and frequencies of the new system. This is a straightforward step as we just use the MATLAB® function `eig( )` to compute the eigenvalues (seen in Tables 4 and 5) and eigenvectors which are used to determine the displacements. Indeed, we project the eigenvectors into displacements using the previous modal shapes as shown by the following relation:

$$\Phi_{\text{new}} = \Phi_{\text{old}}\, \boldsymbol{\phi}$$

Mode	1	2	3	4	5	6	7
Frequency [Hz]	3.50	4.33	5.87	14.08	15.06	29.04	31.40

Table 4: Eigenfrequencies (Modes 1 to 7)

Mode	8	9	10	11	12	13	14
Frequency [Hz]	40.63	44.18	65.28	83.77	91.77	96.28	99.85

Table 5: Eigenfrequencies (Modes 8 to 14)

Remark: As we can see form the tables, the 1st mode is no longer a rigid body mode, therefore characterized by a 0 Hz frequency but rather it has become an elastic mode. Indeed, by introducing an actuator stiffness, the aileron in no longer free to rotate and a rotation leads to the "activation" of the actuator stiffness.

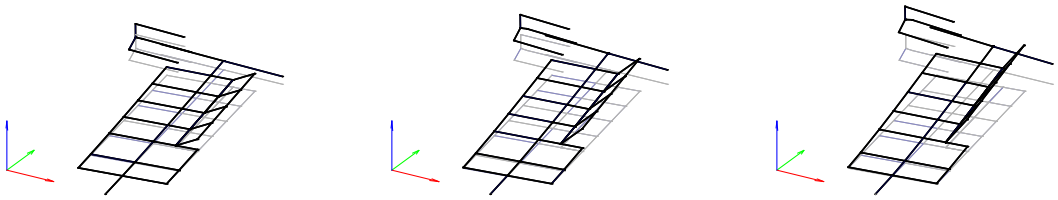

Figure 6: 1st mode shape

Remark: The matrix $\mathbf{K}_{\text{act}_{\text{modal}}}$ is a full 14×14 matrix, meaning that the actuator stiffness impacts is spread throughout all modes. Despite this some modes are not affected by the aileron stiffness. In particular the eigenfrequency associated with the 3rd mode, which is a pure in plane bending, it is not influenced by the actuator stiffness. This can be be explained by the fact the degree of freedom related to the rotation of the aileron is almost uncoupled with respect to the in plane bending degree of freedom.

Task 4: Sensitivity analysis with respect to actuator stiffness

Starting from what was exposed in Task 3, it is possible to analyze how the system reacts to different values of the actuator stiffness. The range we chose for the variation of this parameter is between 0 and $10^{6\,\text{Nm}/\text{rad}}$.

The sensitivity analysis was performed by looking at the behavior of the first 6 modes' eigenfrequencies of the system with respect to different values of the actuator stiffness. As shown in Figure 7, for a stiffness value of 20000 $^{\mathrm{Nm}}/_{\mathrm{rad}}$, there is an intersection between the eigenfrequencies of the second and third modes. In the range of $6000^{\mathrm{Nm}}/_{\mathrm{rad}} - 10000^{\mathrm{Nm}}/_{\mathrm{rad}}$ and $35000^{\mathrm{Nm}}/_{\mathrm{rad}} - 45000^{\mathrm{Nm}}/_{\mathrm{rad}}$ the eigenfrequencies of respectively the first and second modes, and the forth and fifth mode get close together but not intersect. This condition should be avoided because the proximity of two eigenfrequencies can lead to dynamic instabilities.

Remark: In general, the value of the frequencies of the modes influenced by $\mathrm{K_{act}}$ increase as $\mathrm{K_{act}}$ becomes larger. This behavior is physically justified, as a stiffer structure tends to return to its original position "more quickly".

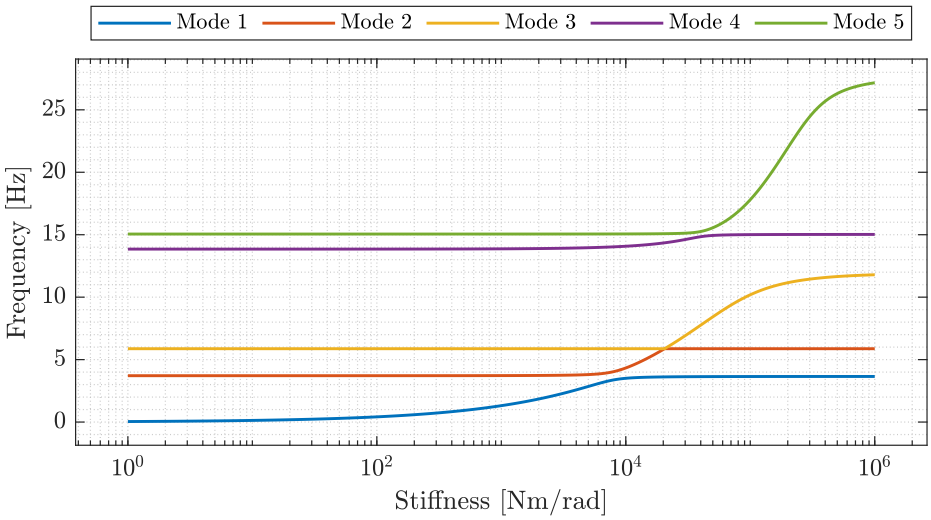

Figure 7: Sensitivity Analysis

Task 5: Mode shapes with actuator damping

Recalling the following equation for the dynamics of the overall system:

$$\mathbf{M}_{hh}\ddot{\mathbf{q}}_h + (\mathbf{C}_{hh} + \mathbf{C}_{hha})\dot{\mathbf{q}}_h + (\mathbf{K}_{hh} + \mathbf{K}_{hha})\mathbf{q}_h = \mathbf{0}$$

We have a null structure modal damping matrix $\mathbf{C}_{\mathrm{hh}}$, while the aileron modal damping matrix $\mathbf{C}_{\mathrm{hha}}$ is built with the same steps of task 3 for the incorporation of the actuator stiffness in the model.

Therefore, we first build the damping matrix in the local reference frame, considering only the 3 rotational degrees of freedom for each node and considering the self and mutual influence of the damping on the nodes. Then we rotate the components of the matrix from the local reference frame to the global reference frame and finally project the global matrix into the modal coordinates, retrieving the final 14×14 modal damping matrix.

Remark: Because it was not introduced a proportional damping, the corresponding damping matrix in modal coordinates is not diagonal.

In order to compute the eigenfrequencies and the modal shapes of the new system we need to exploit the state space formulation and find the eigenvalues and eigenvectors of matrix $\mathbf{A}$. We create a new state vector containing both the modal displacements and modal velocities $[\mathbf{q}_h, \dot{\mathbf{q}}_h]^T$ and as a consequence we recover the following matricial equation:

$$\begin{bmatrix}\dot{\mathbf{q}}_h \\ \ddot{\mathbf{q}}_h\end{bmatrix} = \begin{bmatrix}\mathbb{I} & \mathbf{0} \\ \mathbf{M}^{-1}\mathbf{K} & \mathbf{M}^{-1}\mathbf{C}\end{bmatrix}\begin{bmatrix}\dot{\mathbf{q}}_h \\ \ddot{\mathbf{q}}_h\end{bmatrix} \quad \Longleftrightarrow \quad \dot{\mathbf{Q}}_h = \mathbf{A}\mathbf{Q}_h$$

Using the MATLAB® function `eig( )` we find the 28 eigenvalues and 28 eigenvectors. This is double the number of the original modes as we have the 14 eigenvalues for the displacements and 14 for the velocities.

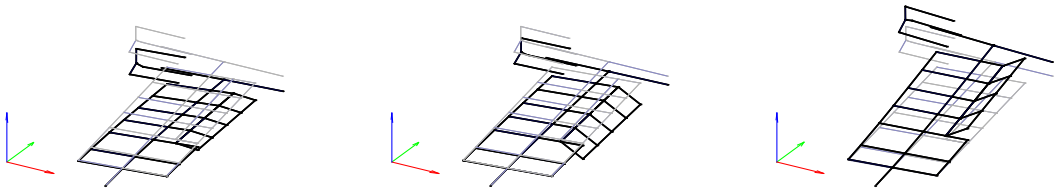

Figure 8: First Mode Shape

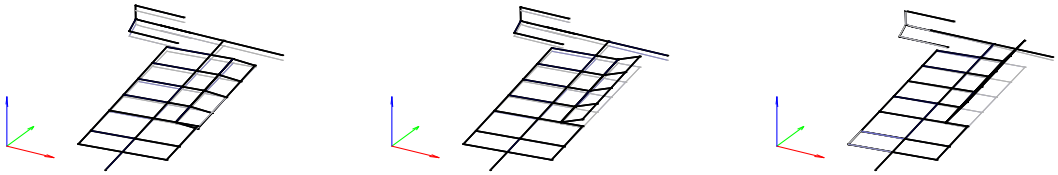

Figure 9: Second Mode Shape

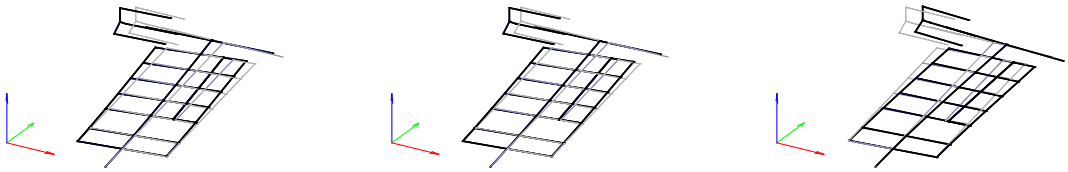

Figure 10: Third Mode Shape

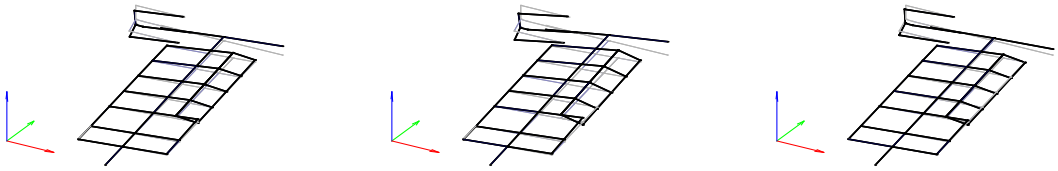

Figure 11: Fourth Mode Shape

Remark: With the introduction of damping the eigenvectors become complex and this is representative of a phase shift between the various modes. This add complexity in the evaluation of the displacements of the nodes. Indeed, considering that the eigenvector components are complex conjugate pairs, the displacement is given by the sum of two eigenvector complex conjugate pairs scaled by the respective eigenvalue:

$$(v_{ij} + \bar{v}_{ij})\lambda_i = \text{real}\left((A + iB)e^{(s+i\omega)t} + (A - iB)e^{(s+i\omega)t}\right) = \ \ldots \ = 2\left(A\cos(\omega t) - B\sin(\omega t)\right)e^{st}$$

Because we want to plot the modes not considering scaling terms, and because the term e^{st} is just a time varying scaling constant, we can omit this term when plotting the modes.

Task 6: Integrating aerodynamics

To integrate aerodynamics in the model inside the MATLAB® environment, we exploit the Roger's approach to write the non linear frequency response function $\mathbf{H}_{am}(k, M)$ into a state space formulation which can be integrated in the previous model. Roger's approach for the state space modeling of aerodynamics is based on the two following equation, where $\mathbf{x}_a$ is the vector of aerodynamics states (42 states for the model that was provided us):

$$\frac{c}{2V_\infty}\dot{\mathbf{x}}_a = \mathbf{A}^{\text{aero}}\mathbf{x}_a + \mathbf{B}^{\text{aero}}\mathbf{q}_h$$

$$\frac{\mathbf{F}_a}{q_\infty} = \mathbf{C}^{\text{aero}}\mathbf{x}_a + \mathbf{D}_0^{\text{aero}}\mathbf{q}_h + \frac{c}{2V_\infty}\mathbf{D}_1^{\text{aero}}\dot{\mathbf{q}}_h + \left(\frac{c}{2V_\infty}\right)^2 \mathbf{D}_2^{\text{aero}}\ddot{\mathbf{q}}_h$$

Integrating this system with the previous structural model, and displaying it into state space form results in the following matricial equation:

$$\left[\begin{array}{c|c|c} \mathbb{I} & \mathbf{0} & \mathbf{0} \\ \mathbf{0} & \mathbf{M}_{hh} - \mathbf{D}_2^{\text{aero}}\, q_\infty \left(\frac{c}{2V_\infty(i)}\right)^2 & \mathbf{0} \\ \mathbf{0} & \mathbf{0} & \mathbb{I} \end{array}\right] \left[\begin{array}{c} \dot{\mathbf{q}}_h \\ \ddot{\mathbf{q}}_h \\ \dot{\mathbf{x}}_a \end{array}\right] = \left[\begin{array}{c|c|c} \mathbf{0} & \mathbb{I} & \mathbf{0} \\ \mathbf{D}_0^{\text{aero}} - \mathbf{K}_{hh}\, q_\infty & \mathbf{D}_1^{\text{aero}} - \mathbf{C}_{hh}\, \frac{c\, q_\infty}{2V_\infty} & \mathbf{C}^{\text{aero}}\, q_\infty \\ \mathbf{B}^{\text{aero}}\, \frac{2V_\infty}{c} & \mathbf{0} & \mathbf{A}^{\text{aero}}\, \frac{2V_\infty}{c} \end{array}\right] \left[\begin{array}{c} \mathbf{q}_h \\ \dot{\mathbf{q}}_h \\ \mathbf{x}_a \end{array}\right]$$

Or in short:

$$\mathbf{V}\,\dot{\mathbf{X}} = \mathbf{A}\,\mathbf{X}$$

In order to perform an aeroelastic analysis in a range of speeds of 100 KTS to 250 KTS, we decided to solve the previous equation with the continuation approach. First we linearize the eigenvalues and eigenvectors in the generalized eigenvalue problem plus and in the normalization condition:

$$(\mathbf{V}\lambda - \mathbf{A})\,\mathbf{q} = 0 \qquad (\mathbf{V}(\lambda_0 + \delta\lambda) - \mathbf{A})(\mathbf{q}_0 + \delta\mathbf{q}) = 0$$

$$\mathbf{q}^T\mathbf{q} = 1 \qquad (\mathbf{q}_0 + \delta\mathbf{q})^T(\mathbf{q}_0 + \delta\mathbf{q}) = 1$$

Based on these equations, we then implement an iterative Newton method to compute for each velocity the eigenvalues and eigenvectors. At each iteration we perform the following computations until both $|\delta\lambda|$ or $\|\delta\mathbf{q}\|$ are below a tolerance or we reach a certain number of iterations.

$$\begin{bmatrix} \mathbf{V}\mathbf{q}_0 & (\mathbf{V}\lambda_0 - \mathbf{A}) \\ \mathbf{0} & 2\mathbf{q}_0^T \end{bmatrix} \begin{bmatrix} \delta\lambda \\ \delta\mathbf{q} \end{bmatrix} = \begin{bmatrix} -(\mathbf{V}\lambda_0 - \mathbf{A})\mathbf{q}_0 \\ 1 - \mathbf{q}_0^T\mathbf{q}_0 \end{bmatrix} \Longrightarrow \text{solve for: } \delta\lambda \text{ and } \delta\mathbf{q}$$

$$\lambda_0(k+1) = \lambda_0(k) + \delta\lambda(k)$$

$$\mathbf{q}_0(k+1) = \mathbf{q}_0(k) + \delta\mathbf{q}(k)$$

As the initial guess for the Newton method we are going to use the structural modes for the initial zero (or small) velocity and for the above velocities we compute the guess in the following way:

$$\begin{bmatrix} \mathbf{V}\mathbf{q}_0 & (\mathbf{V}\lambda_0 - \mathbf{A}) \\ \mathbf{0} & 2\mathbf{q}_0^T \end{bmatrix} \begin{bmatrix} \frac{\partial\lambda}{\partial U} \\ \frac{\partial\mathbf{q}}{\partial U} \end{bmatrix} = \begin{bmatrix} -(\frac{\partial\mathbf{V}}{\partial U}\lambda_0 - \frac{\partial\mathbf{A}}{\partial U})\mathbf{q}_0 \\ 0 \end{bmatrix} \Longrightarrow \text{solve for: } \frac{\partial\lambda}{\partial U} \text{ and } \frac{\partial\mathbf{q}}{\partial U}$$

$$\lambda_{\text{newGuess}} = \lambda_0 + \frac{\partial\lambda}{\partial U}\Delta V_\infty$$

$$\mathbf{q}_{\text{newGuess}} = \mathbf{q}_0 + \frac{\partial\mathbf{q}}{\partial U}\Delta V_\infty$$

In Figure 12, we can see the results of the flutter analysis. By plotting the damping ratio ξ with respect to airspeed, we observe that the damping ratio associated with mode 2 crosses the x-axis at 226.1 KTS (or 116.3 m/s), indicating that this mode encounters a flutter instability.

Flutter instability is a dynamic instability in which the associated eigenvalue is complex and its real part changes from negative to positive. This type of instability is oscillatory in nature, in contrast to divergence, where the phenomenon is static.

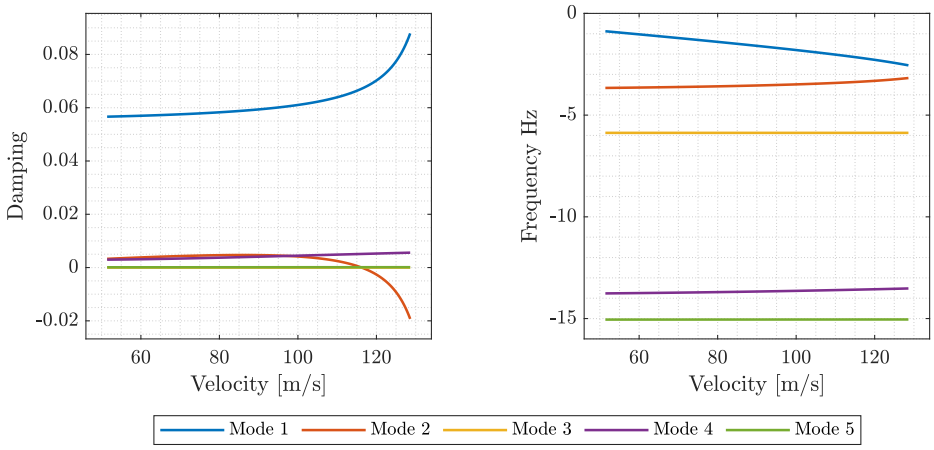

Figure 12: Flutter Analysis

Task 7: Parametric flutter analysis

For this task, we performed a combined parametric analysis by varying the actuator stiffness and damping parameters, evaluating the system's performance across these combinations. The actuator stiffness range is from $0^{\mathrm{Nm}}/_{\mathrm{rad}}$ to $25000^{\mathrm{Nm}}/_{\mathrm{rad}}$ while the actuator damping range is from $0^{\mathrm{Nm}\cdot\mathrm{s}}/_{\mathrm{rad}}$ to $2000^{\mathrm{Nm}\cdot\mathrm{s}}/_{\mathrm{rad}}$. The flutter analysis was then performed using the continuation approach as described in the previous task.

In Figure 13 we have plotted a surface which represents the flutter speed as a function of actuator stiffness and damping. The top and bottom horizontal surfaces represent respectively the upper and lower boundaries of the flight envelope speed. As it can be seen, for low damping and large stiffness (around $25000^{\mathrm{Nm}}/_{\mathrm{rad}}$) the system is flutter free and no value for flutter speed was computed. For large damping (around $2000^{\mathrm{Nm}\cdot\mathrm{s}}/_{\mathrm{rad}}$) and large stiffness values (around $25000^{\mathrm{Nm}}/_{\mathrm{rad}}$) the flutter speed is beyond the maximum operating speed. It is important to mention that flutter speed was searched in the range of airspeeds from $40^{\mathrm{m}}/_{\mathrm{s}}$ to $200^{\mathrm{m}}/_{\mathrm{s}}$.

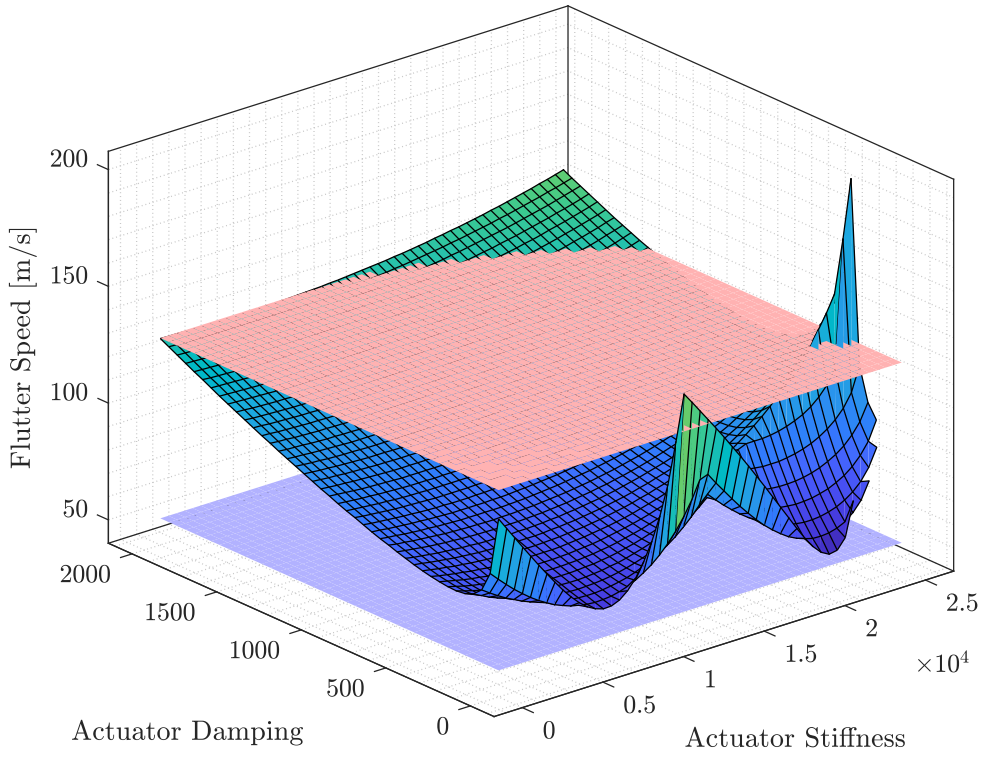

Figure 13: Flutter Analysis

In terms of sensitivity, we can see that for low values of damping, as stiffness increases, we have an irregular and oscillatory pattern of V_{flutter}. For large values of damping the we have instead a much more regular variation of V_{flutter} with respect to stiffness values, and tend to increase. In general, flutter speed first decreases and then increases as damping increases.

Another analysis we performed (as demanded by the task) by artificially building the modal damping matrix with a 3% damping ratio. This meant building a 14×14 diagonal matrix in the following way:

$$\mathbf{C}_{hha} = \text{diag}(2\xi_i \mu_i \omega_i)$$

with $\xi_i = 0.03$; $\mu_i = 1$; and ω_i corresponding to the eigenfrequencies.

In Figure 14 we can see the plot of the damping and eigenfrequencies for varying airspeed. We can see that the system is flutter free for the range of airspeeds in the flight envelope as the damping ratios remain always positive.

Remark: It is interesting to note that the the damping associated with the second mode first increases steadily and then decreases abruptly. This may suggest a possible hard flutter condition for an airspeed above the maximum operating airspeed V_{MO}.

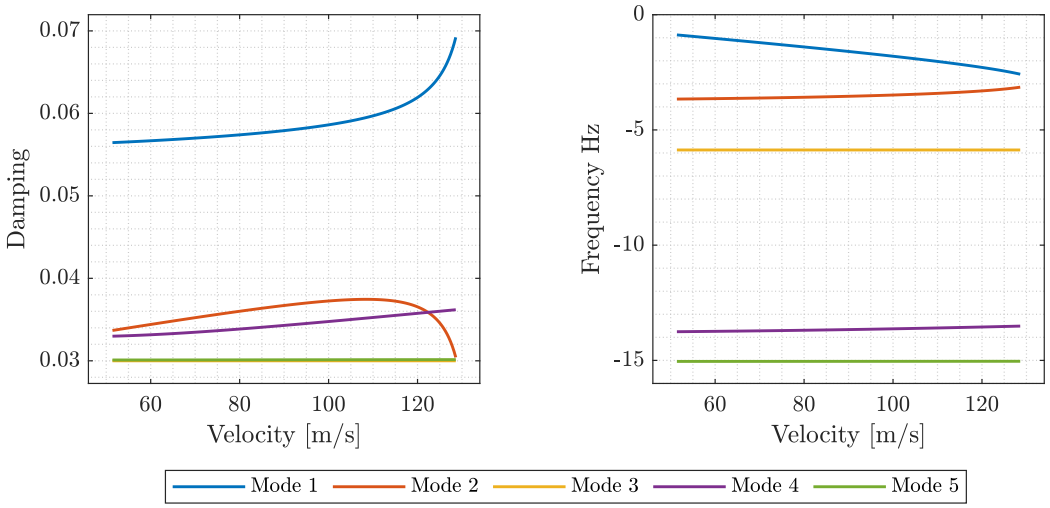

Figure 14: Flutter Analysis with 3% damping

Work partition

The workshop was carried out in full cooperation between the team members. The codes of all tasks were developed and cross-checked together as well as the drafting of the report. For this reason it is not possible to allocate the single contributions of each team member.